

# Evaluation of provenance, tectonic setting, and paleoredox conditions of the Mesoproterozoic–Neoproterozoic basins of the Bastar craton, Central Indian Shield: Using petrography of sandstones and geochemistry of shales

H. Wani<sup>1,†</sup> and M.E.A. Mondal<sup>2</sup>

<sup>1</sup>DEPARTMENT OF GEOLOGY, AMAR SINGH COLLEGE, SRINAGAR 190008, INDIA

<sup>2</sup>DEPARTMENT OF GEOLOGY, ALIGARH MUSLIM UNIVERSITY, ALIGARH 202002, INDIA

## ABSTRACT

We carried out petrographic analyses of the sandstones and geochemical analyses of the shales from the Mesoproterozoic–Neoproterozoic Chhattisgarh and Indravati Basins to determine their tectonic setting, provenance, and paleoredox conditions. Petrographic study shows that the sandstone samples have high amounts of quartz but are depleted in feldspar and lithic fragments. The shales have been classified into the calcareous and noncalcareous shales. The noncalcareous shales have higher concentrations of most of the major elements and trace elements, including the rare earth elements (REEs), in comparison to the calcareous shales. However, this difference in elemental concentrations between the calcareous and noncalcareous shales proved to be significant only for  $\text{SiO}_2$ ,  $\text{TiO}_2$ ,  $\text{Al}_2\text{O}_3$ ,  $\text{MnO}$ ,  $\text{CaO}$ ,  $\text{K}_2\text{O}$ , loss on ignition, Rb, Sr, Nb, Ce, Pr, Sm, Gd, Hf, and Ta using the Student's *t*-test at better than 95% confidence level. Upper continental crust (UCC)–normalized elemental ratios of the calcareous and noncalcareous shales suggest evolved sources similar to UCC. The sandstone petrology and Ni versus Cr diagram, chondrite-normalized REE patterns, and negative  $\text{Eu}/\text{Eu}^*$  values of the calcareous and noncalcareous shale samples reveal that the sediments have been derived from felsic rocks (granites and gneisses) of the Bastar craton. The  $\text{SiO}_2$  versus  $\text{K}_2\text{O}/\text{Na}_2\text{O}$  and  $\text{SiO}_2/\text{Al}_2\text{O}_3$  versus  $\text{K}_2\text{O}/\text{Na}_2\text{O}$  tectonic-setting discrimination diagrams of the shales and the petrology of the sandstones indicate a passive-margin tectonic setting for Chhattisgarh and Indravati Basins. Geochemical parameters such as  $\text{Ce}/\text{Ce}^*$  and  $\text{Mn}^*$  suggest that the calcareous shales were deposited in a suboxic environment, compared to the oxic environment of the noncalcareous shales.

LITHOSPHERE, v. 3, no. 2, p. 143–154.

doi: 10.1130/L74.1

## INTRODUCTION

Precambrian sedimentary rocks are important for understanding the origin and evolution of the continental crust, its composition, Earth's surface processes, tectonic history, and sediment provenance (Wronkiewicz and Condie, 1989; McLennan and Taylor, 1991; Eriksson et al., 1992, 2002). Extensive Mesoproterozoic–Neoproterozoic sedimentary successions, commonly called the Purana succession in Indian stratigraphy (Holland, 1907), occur in seven cratonic basins in the peninsular India—Vindhyan Basin, Cuddapah Basin, Chhattisgarh Basin, Indravati Basin, Pranhita-Godavari Basin, Bhima Basin, and Kaladgi Basin (Fig. 1). These basins occupy large areas of cratonic blocks (Rogers, 1986). These Proterozoic basins are comparable with the Proterozoic basins of North America, Australia, and the Siberian platform with respect to age, duration of basin history, size, sediment thickness, and depositional systems (Preiss and Forbes, 1981; Kale and Phansalkar, 1991; Patranabis Deb, 2004). Among these seven Mesoproterozoic–Neoproterozoic sedimentary basins of the Indian Peninsula, the Chhattisgarh and Indravati Basins occur in the Bastar craton.

A variety of sediments deposited in the Chhattisgarh and Indravati Basins of the Bastar craton have sampled the continental crust of that period and, therefore, act as a repository of evidence and clues regarding the composition of the Proterozoic continental crust, and the tectonic environment prevailing at the time of deposition of the rocks of the Chhattisgarh and Indravati Basins.

Sandstone petrography is widely considered to be a powerful tool for determining the origin and tectonic setting of ancient terrigenous deposits (Blatt, 1967; Dickinson, 1970; Pettijohn et al., 1972). Shale geochemistry has been considered to represent the average crustal composition much better than any other detrital sedimentary rock because of its grain-size homogeneity and postdepositional impermeability (McCulloch and Wasserburg, 1978; Bhat and Ghosh, 2001). Proterozoic shales have been studied in different parts of the world to understand the nature of the upper continental crust, which developed by the close of the Archean (Taylor and McLennan, 1985; Wronkiewicz and Condie, 1990). In the present paper, we studied the petrography of the sandstones and geochemistry of the shales from the Chhattisgarh and Indravati Basins of the Bastar craton to determine their provenance, tectonic setting, and paleoredox conditions. Further, we draw comparisons between present geochemical data on shales and the available geochemical data from NASC (North American Shale Composite; Gromet et al., 1984), UCC (upper continental crust; Taylor and McLennan, 1985), granite and gneiss of the Bastar craton (Mondal et al., 2006), and the Archean mafic volcanic rocks of the Bastar craton (Srivastava et al., 2004) to identify source-rock characteristics.

## GEOLOGICAL SETTING

The Singhbhum, Dharwar, and Bastar nuclei together constitute the southern peninsular block of India (Radhakrishna, 1989). Toward the north, the Bastar craton was accreted with the Aravalli–Bundelkhand

<sup>†</sup>E-mail: hamid79@rediffmail.com.

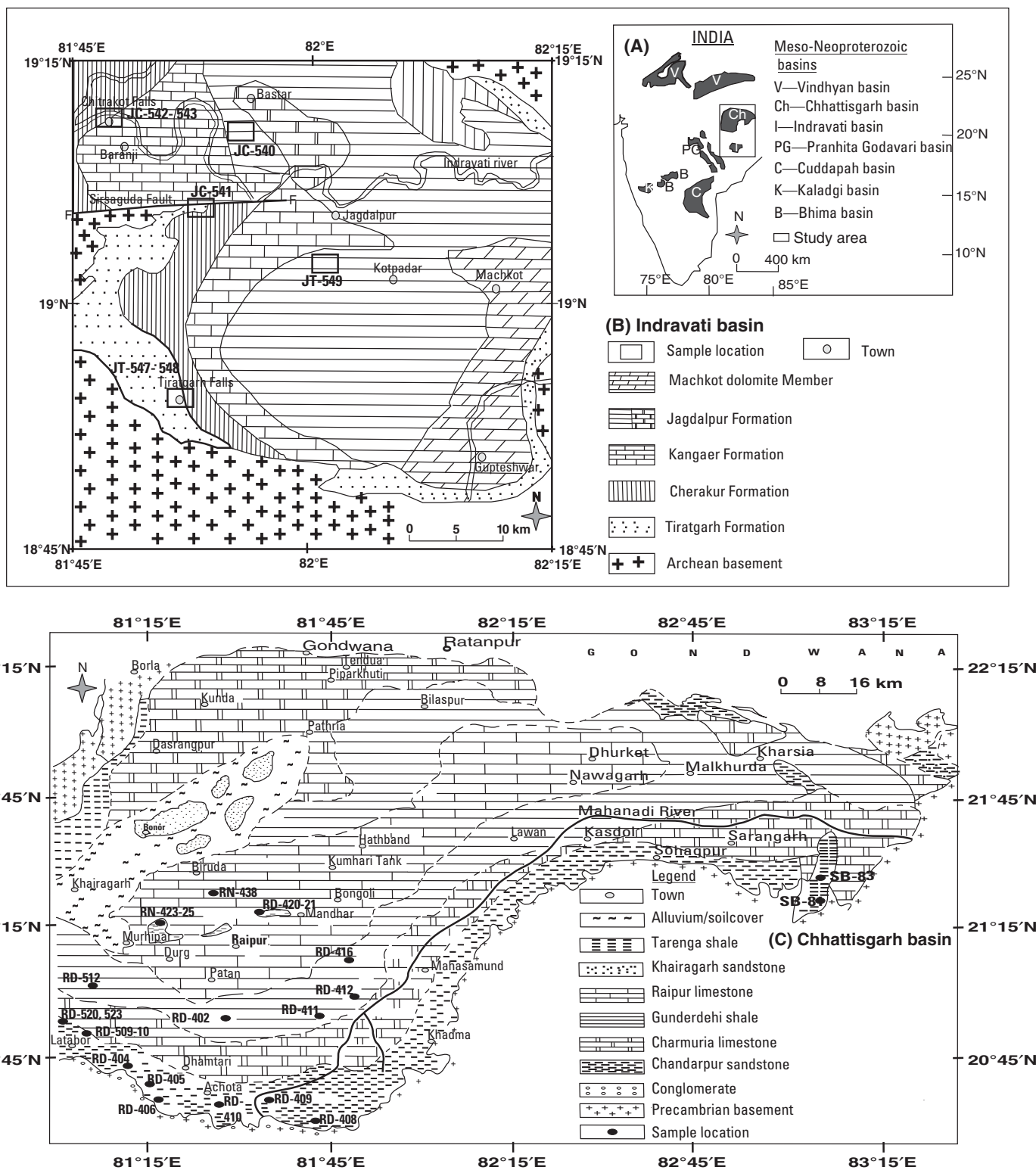


Figure 1. (A) Geological map of India showing distribution of the Mesoproterozoic–Neoproterozoic basins of the Indian peninsula. (B) Geological map of the Indravati Basin (Ramakrishnan, 1987) and (C) geological map of the Chhattisgarh Basin (Murthi, 1987) of the Bastar craton from which samples were taken. Numbers refer to sample locations.

TABLE 1. THE GENERAL STRATIGRAPHIC SUCCESSIONS OF THE CHHATTISGARH AND INDRAVATI BASINS OF THE BASTAR CRATON (NAQVI AND ROGERS, 1987; RAMAKRISHNAN, 1987; MURTHI, 1987)

Formation	Lithology	Depositional environment
<b>Chhattisgarh Basin (Chhattisgarh Supergroup)</b>		
<i>Raipur Group</i>		
Tarenga Formation	Purple shale and purple limestone	Slope to basin Platform margin, slope to basin Platform
Chandi Formation	Gray and pink limestone	
Gunderdehi Formation	Pink and purple shale/gray shale	
Charmuria Formation	Gray limestone/white to buff clays	
<i>Chandrapur Group</i>		
Kansapathar Formation	White sandstone	Shoreface bar and wind flats
Chaporadih Formation	Reddish brown and olive green sandstone	Prodelta and prograding shelf
Lohardih Formation	White pebbly sandstone	Fan-delta complex
Unconformity		
Archean granites, gneisses, and older supracrustals (Sonakhan greenstone belt)		
<b>Indravati Basin</b>		
Jagdalspur Formation	Calcareous shales with purple and gray	Shallow siliciclastic-carbonate shelf
Kanger Limestone	Purple limestone, gray limestone	Deep-water carbonate platform
Cherakur Formation	Purple shale with arkosic sandstone and chert pebble conglomerate, grit	Intertidal to subtidal
Tiratgarh Formation	Chitrakot sandstone member (quartz arenite) Mendri sandstone member (subarkose and conglomerate)	Beach, fan-delta
Unconformity		
Archean granites, gneisses, and older supracrustals (Sonakhan greenstone belt)		

craton along east-northeast– to west-southwest–trending Narmada-Son Lineaments, which together constitute the Central Indian Shield (Bando-padhaya et al., 1995). The Bastar craton lies in the southern corner of the Central Indian Shield. It is bounded on the east by the high-grade Eastern Ghat mobile belt and on the north and south by the Mahanadi and Godavari rifts, respectively. The Chhattisgarh and Indravati Basins of the Bastar craton contain unmetamorphosed conglomerate, sandstone, shale, limestone, chert, and dolomite (Table 1). The age of the Chhattisgarh and Indravati Basins has been assigned to be Mesoproterozoic–Neoproterozoic (Chaudhuri et al., 1999). The origin of the basins of the Bastar craton is poorly constrained, though a riftogenic origin has been invoked for them (Naqvi and Rogers, 1987; Kale and Phansalkar, 1991; Takashi et al., 2001; Chaudhuri et al., 2002).

## METHODOLOGY

In order to represent the maximum possible stratigraphical, spatial, and lithological variations of clastic rocks, fresh sandstone and shale, samples were collected from outcrops and mine sections in the study area. Twenty-one sandstone samples from the Chandrapur Group and the Tiratgarh Formation, which stratigraphically form the lower parts of the Chhattisgarh and Indravati Basins, respectively, were selected for modal analysis (Fig. 2). Mineralogical composition of the sandstones was determined by modal analysis. Point counting was carried out using the Gazzi-Dickinson method (Dickinson, 1970; Le Gazzi, 1966; Ingersoll et al., 1984). More than 500 points were counted for each thin section, using the maximum grid spacing to give full coverage to the thin section slide. Petrographic examinations were done for the shale samples from the point of view of secondary alterations. After careful petrographic studies, shale samples from the Gunderdehi Formation and the Tarenga Formation of the Raipur Group, which stratigraphically form the upper part of the Chhattisgarh Basin, and also the Jagdalspur Formation, which forms the upper part of the Indravati Basin (Fig. 2), were selected for geochemical analysis to obtain analytical data for major, trace, and rare earth elements (REEs).

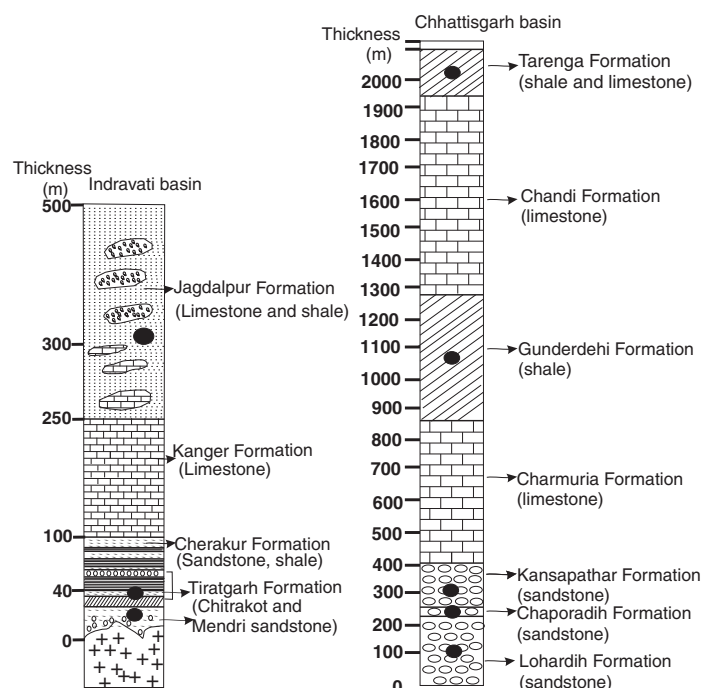


Figure 2. Stratigraphic column of the Indravati and Chhattisgarh Basins showing the rock formations (indicated by dark circles) from which the samples were taken.

Major elements were analyzed on WD-XRF (Wavelength Dispersive X-Ray Fluorescence Spectrometer) (Siemens SRS 3000) at the Wadia Institute of Himalayan Geology, Dehradun, India. The precision of XRF major oxide data is better than 1.5%. Details of the analytic techniques and precision and accuracy of the instrument are described in Saini et

al. (1998). Trace elements, including REEs, were analyzed on an inductively coupled plasma–mass spectrometer (ICP-MS) (Perkin Elmer Sciex ELAN DRC II) at the National Geophysical Research Institute, Hyderabad, India. The precision of ICP-MS trace-element and REE data is better than 5%. Details of the analytic techniques and accuracy and precision of the instrument are described in Roy et al. (2007).

## RESULTS

### Petrography of Sandstones

#### Chandarpur Group (Chhattisgarh Basin)

**Lohardih Formation.** Sandstones of the Lohardih Formation are dominated by quartz (71% on average). Monocrystalline quartz is a dominant type, averaging 68%. Feldspar content of this formation exceeds that of any other formation documented here, and the entire feldspar population

averages 4% for the sample set. Microcline dominates over plagioclase. The P/K ratio (plagioclase/ K-feldspar ratio) averages 0.5. The rock fragments in these sandstones are made up of chert, and this stratigraphic unit has the highest representation of chert grains (5% on average) (Table 2).

**Chaporadih Formation.** Sandstones of the Chaporadih Formation are characterized by high values of quartz (82% on average). Quartz is strongly dominated by monocrystalline quartz, with an average of 77%. Polycrystalline quartz generally constitutes 5% of quartz grains. Microcline dominates over plagioclase (P/K ratio averages 0.25). Glauconite pellets are very common in the Chaporadih Formation (up to 11%) (Table 2). The cementing material is mostly silica cement (quartz overgrowth).

**Kansapathar Formation.** Sandstones of this stratigraphic unit have the highest amount of quartz grains (average 95%). The framework grains of sandstones of the Kansapathar Formation are composed dominantly of monocrystalline and polycrystalline quartz, with insignificant feldspar and rock fragments, including chert, which is 1% on average. Stretched

TABLE 2. SANDSTONE COMPOSITIONS OF THE CHANDARPUR GROUP OF THE CHHATTISGARH BASIN AND THE TIRATGARH FORMATION OF THE INDRAVATI BASIN

Sample no.	Qm (%)	Qp (%)	K-feldspar (%)	Plagioclase (%)	Feldspar total (%)	Chert (%)	Glauconite (%)	Silica cement (%)	Calcite cement (%)	Iron cement (%)	Rock fragment (%)	Others (%)	Total (%)
<b>Chandarpur Group</b>													
<i>Lohardih Formation</i>													
RD-406	76.33	5.12	6.18	3.18	9.36	0	0	0.55	6.53	0.7	1.23	0.18	100
RD-420	37.46	0.65	0.65	1.6	2.25	9.65	0	0.16	33.44	16.07	0	0.32	100
RD-421	57.64	1.05	1.91	0.52	2.43	4.68	0	0.52	33.15	0.35	0	0.18	100
RN-438	79.37	3.37	2.52	1.05	3.57	6.53	0	5.06	0	1.05	0	1.05	100
RD-509	85.9	4.51	0.37	0	0.37	6.02	0	2.07	0	0.94	0	0.19	100
RD-523	68.36	5.68	3.84	1.38	5.22	3.32	0	0	15.55	0.3	0.77	0.8	100
Average	68	3	3	1	4	5	0	1	15	3	0.5	0.5	100
Average P/K ratio of the Lohardih Formation is 0.5													
<i>Chaporadih Formation</i>													
RD-404	80.47	9.19	1.34	0	1.34	2	3.01	0.66	0	0.83	1.83	0.67	100
RN-423	67.26	4.19	0	0	0	3.07	21.77	2.09	0	1.45	0	0.17	100
RN-425	82.01	1	2.02	0.86	2.88	2.44	9.06	1.73	0	0.59	0	0.29	100
Average	77	5	1	0.3	1.4	2.5	11	1.5	0	0.6	0.7	0.4	100
Average P/K ratio of the Chaporadih Formation is 0.25													
<i>Kansapathar Formation</i>													
RD-405	87.28	6.66	0	0	0	2.37	0	2.52	0	0.29	0	0.88	100
RD-408	86.76	3.63	0.9	0.55	1.45	0.72	0	1.99	0	5.27	0	0.18	100
RD-409	91.54	4.94	0	0	0	0.58	0	2.12	0	0.23	0.36	0.23	100
RD-410	80	16.5	0	0	0	2.17	0	0.49	0	0.24	0.24	0.36	100
RN-424	88.89	5.48	0.81	0	0.81	0.16	0	4.02	0	0.32	0	0.32	100
RD-510	85.33	7.81	0	0	0	2.43	0	1.14	0	0.72	2.28	0.29	100
RD-520	93.79	1.77	0	0	0	0	0	4.14	0	0.15	0	0.15	100
Average	88	7	0.2	0.1	0.3	1	0	2	0	1	0.4	0.3	100
Average P/K ratio of the Kansapathar Formation is 0.3													
Average of all the three formations of the Chandarpur Group:													
	77	5	1.4	0.4	2	2.5	3	1.5	5	1.3	0.5	0.4	100
Average P/K ratio of all the three formations of the Chandarpur Group is 0.44													
<b>Indravati Group</b>													
<i>Tiratgarh Formation</i>													
JC-541	3.28	85.8	5.47	1.09	6.56	0	0	0	3.83	0.18	0	0.35	100
JC-542	79.83	1.8	0.36	1.26	1.62	3.61	0	0.36	10.61	0.9	0.54	0.73	100
JC-543	89.79	5.83	0	0	0	0	0	0.36	3.05	0.36	0.48	0.13	100
JT-547	50.42	32.1	1.53	0.41	1.94	2.08	0	0	10.42	1.12	1.38	0.54	100
JT-548	86.14	5.82	0	0	0	5.54	0	1.25	0	0.69	0.28	0.28	100
Average	62	26	1.5	0.6	2	2	0	0.4	6	0.6	0.5	0.4	100
Average P/K ratio of the Tiratgarh Formation is 0.37													
Note: Qm—monocrystalline quartz, Qp—polycrystalline quartz, P/K—plagioclase/K-feldspar. Others include heavy minerals and mica.													

metamorphic quartz is very common among the polycrystalline quartz. The intragranular space is entirely filled with the quartz cement, which constitutes ~2% on average (Table 2).

### Indravati Group (Indravati Basin)

**Tiratgarh Formation.** Sandstones of the Tiratgarh Formation of the Indravati Group are also dominated by quartz (88% on average). Monocrystalline is the dominant quartz type (62% on average); however, in two samples, polycrystalline quartz dominates. K-feldspar dominates over plagioclase, except in one sample (P/K ratio averages 0.37), and the entire feldspar population averages 2% for all samples (Table 2). The sandstones are mainly cemented by carbonate and silica minerals. Heavy minerals and opaques are rare and are dominated by zircon and iron oxides, respectively. Quartz cement occurs primarily as overgrowth around quartz grains. Rock fragments are rare and are dominated by chert fragments.

The general petrographic attributes show similarity between the Lohardih Formation and the Tiratgarh Formation, which form the basal part of the Chandarpur Group and the Indravati Group, respectively. These formations are somewhat feldspathic and weakly quartz cemented. The decreasing feldspar content at the top of the Chandarpur Group (Kansapathar Formation) is accompanied by a corresponding increase in the framework quartz as well as quartz cement. Monocrystalline and polycrystalline quartz varieties exhibit a positive correlation in their contents. The frequency of feldspar gradually declines while monocrystalline quartz and polycrystalline quartz increase upward at the top of the Kansapathar Formation and the rock becomes a supermature quartz-arenite with quartz cement up to 2.34%.

### Geochemistry of Shales

#### Major Elements

Petrographic observation reveals that the shales of the Bastar craton display compositional variation, from calcite-rich shale to a typical shale. This is best depicted by the abundance of CaO concentrations in these shales. Therefore, we can classify the shale samples of the Gunderdehi Formation of the Chhattisgarh Basin into calcareous shales (>6% CaO) and the shale samples of the Tarenga Formation of the Chhattisgarh Basin and the Jagdalpur Formation of the Indravati Basin into noncalcareous shales (<0.3% CaO). The major elements and trace elements, including REE data of the shale samples, are given in Table 3.

In comparison to NASC, the noncalcareous shales are enriched in  $\text{Al}_2\text{O}_3$ ,  $\text{Fe}_2\text{O}_3$ , and  $\text{K}_2\text{O}$  and slightly depleted in other elements (Fig. 3). The calcareous shales are enriched in CaO and MnO and depleted in other elements. The mean concentrations of major elements in the calcareous shales are characterized by lower values of  $\text{SiO}_2$  and higher values of CaO compared to the noncalcareous shales. Mean values of immobile elements like  $\text{Al}_2\text{O}_3$ ,  $\text{TiO}_2$ , and  $\text{Fe}_2\text{O}_3$  are higher in the noncalcareous shales compared to the calcareous shales. Mean values of mobile elements like  $\text{K}_2\text{O}$  are higher in the noncalcareous shales compared to the calcareous shales. This difference in major-element compositions between the shales has proved to be significant for  $\text{SiO}_2$ ,  $\text{TiO}_2$ ,  $\text{Al}_2\text{O}_3$ ,  $\text{Fe}_2\text{O}_3$ , MnO, CaO,  $\text{K}_2\text{O}$ , and loss on ignition using the Student's *t*-test at better than 95% confidence level ( $p < 0.05$ ) (Table 3).

#### Trace Elements

In comparison to NASC, the noncalcareous shales are enriched in Rb, Cs, Th, Ta, and Nb and are slightly depleted in other trace elements. The calcareous shales are enriched in Sr, Cs, Ba, and Th and strongly depleted in most of the trace elements compared to the NASC. In comparison to the calcareous shales, the noncalcareous shales have higher mean values of

transition elements like Cr and Ni. In both the calcareous and noncalcareous shales,  $\text{Al}_2\text{O}_3$  shows positive correlation with most of the transition elements, like Cr ( $r = 0.99$  for the calcareous shales and  $r = 0.77$  for the noncalcareous shales), indicating their clay mineral control. Mean values of large ion lithophile elements (LILEs), such as Rb and Cs, and high field strength elements (HFSEs), such as Th, Zr, Hf, Nb, and U, of the noncalcareous shales are higher as compared to the calcareous shales. Exceptions are the values of Ba, Sr, and Y, which are higher in the calcareous shales. However, the difference in trace-element concentrations between the calcareous and the noncalcareous shales is insignificant for Sc, V, Cr, Co, Ni, Y, Zr, Sc, and Ba, while it is significant for Rb, Sr, Nb, Hf, and Ta using the Student's *t*-test at better than 95% confidence level ( $p < 0.05$ ) (Table 3).

#### Rare Earth Elements

In comparison to NASC, the noncalcareous shales have higher REE abundances compared to the calcareous shales. Total REE ( $\Sigma\text{REE}$ ) concentrations are variable in the shale samples, with higher mean value in noncalcareous shales (263 ppm) and lower value in the calcareous shales (180 ppm). The difference in REE concentrations between the calcareous and noncalcareous shales has been found to be significant for elements such as Ce, Pr, Nd, and Gd using the Student's *t*-test at better than 95% confidence level ( $p < 0.05$ ) (Table 3). On the chondrite-normalized REE diagram (Sun and McDonough, 1989) (Fig. 4), light (L) REE patterns of the noncalcareous and calcareous shales are fractionated, with LREE enrichment ( $\text{La/Yb}_n = 19.1$  for the noncalcareous shales and 6.71 for the calcareous shales, flat heavy (H) REE ( $\text{Gd/Yb}_n = 1.95$  for the noncalcareous shales and 1.35 for the calcareous shales, and a significant negative Eu anomaly ( $\text{Eu/Eu}^* = 0.61$  for the noncalcareous shales and 0.81 for the calcareous shales).

### DISCUSSION

#### Tectonic Setting

The Bastar craton of the Central Indian Shield and its Proterozoic sedimentary basins are very significant with regard to Proterozoic tectonic evolution. There has not been any significant study of the Proterozoic tectonic evolution of the Chhattisgarh and Indravati Basins of the Bastar craton using petrography and geochemistry of clastic rocks. Sandstone petrography is widely considered to be a powerful tool for determining the origin and tectonic setting of ancient terrigenous deposits (Blatt, 1967; Dickinson, 1970; Pettijohn et al., 1972). Quite a few of the standard methods for analyzing petrographical and geochemical data of clastic rocks are essentially based on Phanerozoic data sets. Applications of these methods to Precambrian rocks have to be made with some caution, because one cannot always assume uniformity in tectonic styles between the Precambrian and Phanerozoic. However, a recent study by Cawood et al. (2006) using paleomagnetic, geochemical, and tectonostratigraphic data established that plate tectonics have been active since at least 3.1 Ga, and the tectonic regime of Precambrian lithospheric plates was similar to Phanerozoic Earth. In the absence of standard methods for unraveling crustal evolution processes based on petrological and geochemical data of Precambrian sedimentary rocks, we employed techniques and methods based on Phanerozoic data sets for our rocks of Precambrian age.

To identify the provenance and tectonic setting of the sandstone samples, the recalculated parameters of Folk (1980) and Dickinson and Suczek (1979) were plotted on standard ternary diagrams given by Dickinson and Suczek (1979). In the QtFL diagram (Dickinson and Suczek, 1979) (Fig. 5A), most of the sandstone samples of the Lohardih Formation, the Chaporadih Formation, and the Kansapathar Formation of the Chandarpur Group, and the Tiratgarh Formation of the Indravati Group, plot in

TABLE 3. CHEMICAL COMPOSITIONS OF THE CALCAREOUS AND NONCALCAREOUS SHALES OF THE CHHATTISGARH AND INDRAVATI BASINS

Sample number	Calcareous shales							Noncalcareous shales							Mean difference	t value	P value
	Gunderdehi Formation (CB)					Mean	Std	Tarenga Formation (CB)		Jagdalpur Formation (IB)		Mean	Std				
	RD402	RD411	RD412	RD416	RD512			SB81	SB83	JC540	JT549						
<b>Major elements (wt%)</b>																	
SiO <sub>2</sub>	56.71	50.28	37.77	39.93	29.03	42.74	10.86	73.86	70.05	58	54.07	63.99	9.45	-21.25	-3.1	0.018	
TiO <sub>2</sub>	0.6	0.5	0.29	0.36	0.29	0.4	0.13	0.63	0.65	0.74	0.76	0.69	0.06	-0.29	-3.8	0.007	
Al <sub>2</sub> O <sub>3</sub>	14.23	12.82	8.01	9.37	7.01	10.28	3.11	11.93	18.27	18.59	20.04	17.2	3.6	-6.92	-3.1	0.017	
Fe <sub>2</sub> O <sub>3</sub> *	5.33	4.27	2.59	2.78	1.66	3.32	1.45	6.7	3.89	7.95	11.04	7.39	2.96	-4.07	1.64	0.144	
MnO	0.06	0.06	0.06	0.07	0.04	0.05	0.01	0.02	0.02	0.02	0.01	0.01	0.005	0.04	6.78	0	
MgO	2.02	2.03	1.44	1.64	1.08	1.64	0.4	1.33	0.86	1.66	1.19	1.26	0.33	0.38	1.52	0.172	
CaO	6.84	9.27	26.51	27.25	35.07	20.98	12.3	0.28	0.07	0.04	0.04	0.1	0.11	20.88	3.35	0.012	
Na <sub>2</sub> O	0.34	0.38	0.11	0.26	0.02	0.22	0.15	0.15	0.37	0.14	0.12	0.19	0.11	0.03	0.29	0.78	
K <sub>2</sub> O	3.72	3.56	2.07	2.48	1.39	2.64	0.99	4.47	4.18	6.51	6.81	5.49	1.35	-2.85	-3.7	0.008	
P <sub>2</sub> O <sub>5</sub>	0.08	0.1	0.12	0.1	0.07	0.09	0.01	0.14	0.04	0.07	0.06	0.07	0.04	0.02	0.77	0.468	
LOI	10.06	15.98	20.42	15.34	24.2	17.2	5.36	0.52	1.2	6.26	5.46	3.36	2.91	13.84	4.6	0.002	
Total	99.99	99.25	99.39	99.58	99.86	ND	ND	100	99.6	99.98	99.6	ND	ND	ND	ND	ND	
<b>Trace and rare earth elements (REEs) (ppm)</b>																	
Sc	17.4	15.7	13.3	13.3	7.3	13.4	3.8	11.7	16.1	14.8	16.7	14.8	2.231	-1.4	-0.6	0.543	
V	96.3	98.3	62.9	69.0	33.1	71.9	26.84	59.4	95.3	80.5	90.7	81.5	15.95	-9.6	-0.6	0.552	
Cr	81.6	67.1	41.8	51.1	31.1	54.5	20.06	50.8	63.3	119.1	134.3	91.9	41.02	-37.4	-1.8	0.114	
Co	16.3	17.3	15.5	12.6	3.2	13.0	5.725	13.4	9.6	14	5.4	10.6	3.975	2.4	0.71	0.502	
Ni	38.9	36.9	28.8	30.9	8.6	28.8	12.05	43.5	23	38.8	50.8	39	11.76	-10.2	-1.3	0.242	
Rb	175.9	153.6	93.6	111.3	64.8	119.8	44.91	159.7	198.2	228.1	316.4	225.6	66.7	-105.8	-2.9	0.025	
Sr	89.0	147.5	200.7	211.6	181.5	166.1	49.48	43	57.8	22.9	33.5	39.3	14.8	126.8	4.89	0.002	
Y	27.3	26.1	25.1	26.0	17.9	24.5	3.781	15.2	30	24.4	21.9	22.9	6.112	1.6	0.49	0.667	
Zr	144.4	118.1	71.3	85.1	54.9	94.7	36.18	240.7	179.6	3.1	189.5	153.2	103.6	-58.5	-1.2	0.272	
Nb	12.9	10.2	6.9	8.2	5.6	8.7	2.881	37.2	17.1	19.6	19.5	23.3	9.291	-14.6	-3.4	0.012	
Cs	13.0	10.0	6.0	7.8	6.7	8.7	2.838	11.8	10.9	12.3	16.4	12.9	2.414	-4.2	-2.3	0.052	
Ba	2091.3	427.6	4255.7	2515.5	1.4	1858.0	1712	412.7	528.9	495.9	0.9	359.6	244.1	1498	1.71	0.13	
La	31.5	25.4	24.3	22.4	18.0	24.3	4.888	44.8	56.3	69.9	101	68	24.28	-43.7	-4	0.005	
Ce	63.4	52.8	43.7	43.9	20.5	44.9	15.86	93.8	100	112.7	131.2	109.4	16.48	-64.5	-6	0.001	
Pr	8.7	7.2	6.2	6.3	3.4	6.4	1.932	9.7	12.6	13.3	16.8	13.1	2.887	-6.7	-4.2	0.004	
Nd	32.3	27.7	24.1	24.8	12.6	24.3	7.286	34.5	45.5	45.5	55	45.1	8.384	-20.8	-4	0.005	
Sm	6.6	5.8	5.7	5.7	3.5	5.4	1.173	5.7	8.3	7.8	8.9	7.7	1.353	-2.3	-2.6	0.033	
Eu	1.3	1.1	1.4	1.3	1.0	1.2	0.176	1	1.5	1.4	1.5	1.3	0.261	-0.1	-0.2	0.384	
Gd	5.2	4.7	4.4	4.5	2.5	4.2	1.022	4.4	6.5	6.7	6.5	6	1.104	-1.8	-2.5	0.047	
Tb	0.9	0.8	0.7	0.7	0.4	0.7	0.162	0.6	1	1	0.9	0.9	0.187	-0.2	-1.6	0.164	
Dy	4.9	4.5	4.4	4.4	2.8	4.2	0.835	3.3	5.7	5.2	4.4	4.7	1.035	-0.5	-0.7	0.505	
Ho	1.0	0.9	0.9	0.8	0.6	0.8	0.142	0.6	1.1	1	0.8	0.9	0.25	-0.1	-0.4	0.712	
Er	2.8	2.6	2.4	2.4	1.7	2.4	0.4	1.6	3.3	2.7	2.4	2.5	0.693	-0.1	-0.3	0.743	
Tm	0.4	0.4	0.4	0.4	0.3	0.4	0.063	0.2	0.5	0.4	0.4	0.4	0.12	0	-0	0.962	
Yb	2.9	2.9	2.5	2.6	1.9	2.5	0.402	1.5	3.5	2.7	2.7	2.6	0.818	-0.1	-0.2	0.872	
Lu	0.4	0.4	0.4	0.4	0.3	0.4	0.063	0.2	0.5	0.4	0.4	0.4	0.132	0	-0.1	0.896	
Hf	4.4	3.5	2.2	2.6	1.7	2.9	1.064	6.5	5.5	6.4	6.2	6.1	0.418	-3.2	-5.7	0.001	
Ta	1.4	1.1	1.4	0.8	0.4	1.0	0.442	2.8	2	1.5	1.5	1.9	0.613	-0.9	-2.6	0.033	
Th	18.7	15.1	11.3	12.4	7.8	13.0	4.095	12.3	19.5	29.9	31.5	23.3	9.089	-10.3	-2.3	0.057	
U	2.3	2.1	1.4	1.6	0.6	1.6	0.656	1.1	2.6	1.4	1.4	1.6	0.678	0	-0.1	0.936	
Eu/Eu*	0.7	0.65	0.87	0.8	1.04	0.812	ND	0.6	0.64	0.6	0.61	0.613	ND	ND	ND	ND	
(La/Yb) <sub>n</sub>	7.66	6.28	6.9	6.09	6.66	6.718	ND	20.37	11.31	18.58	26.17	19.11	ND	ND	ND	ND	
(Gd/Yb) <sub>n</sub>	1.47	1.34	1.44	1.42	1.08	1.35	ND	2.3	1.51	2.06	1.95	1.955	ND	ND	ND	ND	
Ce/Ce*	0.93	0.95	0.86	0.9	0.63	0.854	ND	1.09	0.91	0.9	0.78	0.92	ND	ND	ND	ND	
Mn*	-0.01	0.07	0.29	0.33	0.31	0.198	ND	-0.59	-0.35	-0.66	-1.11	-0.68	ND	ND	ND	ND	

Note: Total iron as Fe<sub>2</sub>O<sub>3</sub>\*; LOI—loss on ignition; CB—Chhattisgarh Basin; IB—Indravati Basin; ND—not determined; Std—standard deviation.

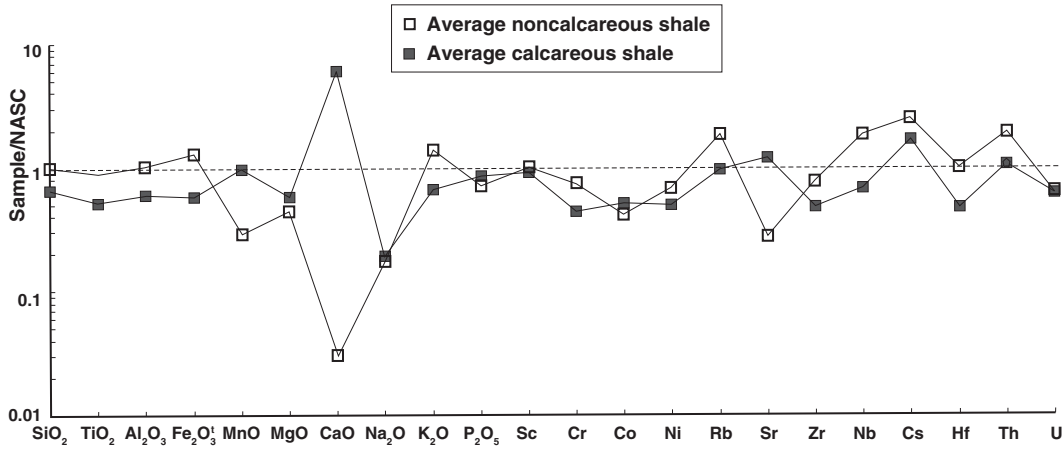


Figure 3. NASC (North American shale composite)-normalized average major- and trace-element composition of the calcareous and non-calcareous shales. NASC values are from Gromet et al. (1984).

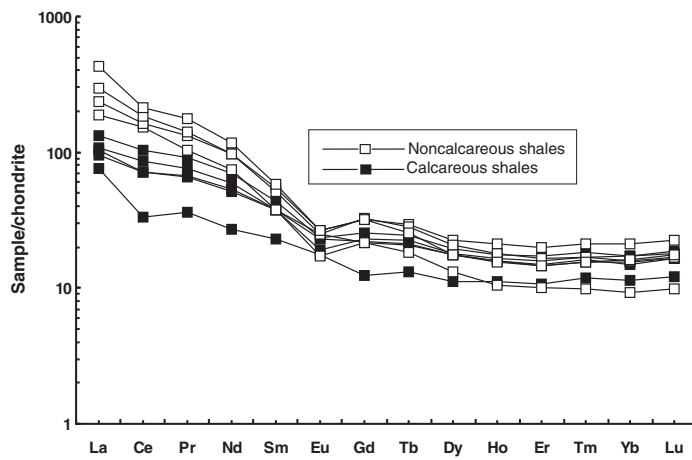


Figure 4. Chondrite-normalized rare earth element (REE) patterns of the calcareous and noncalcareous shales of the Chhattisgarh and Indravati Basins.

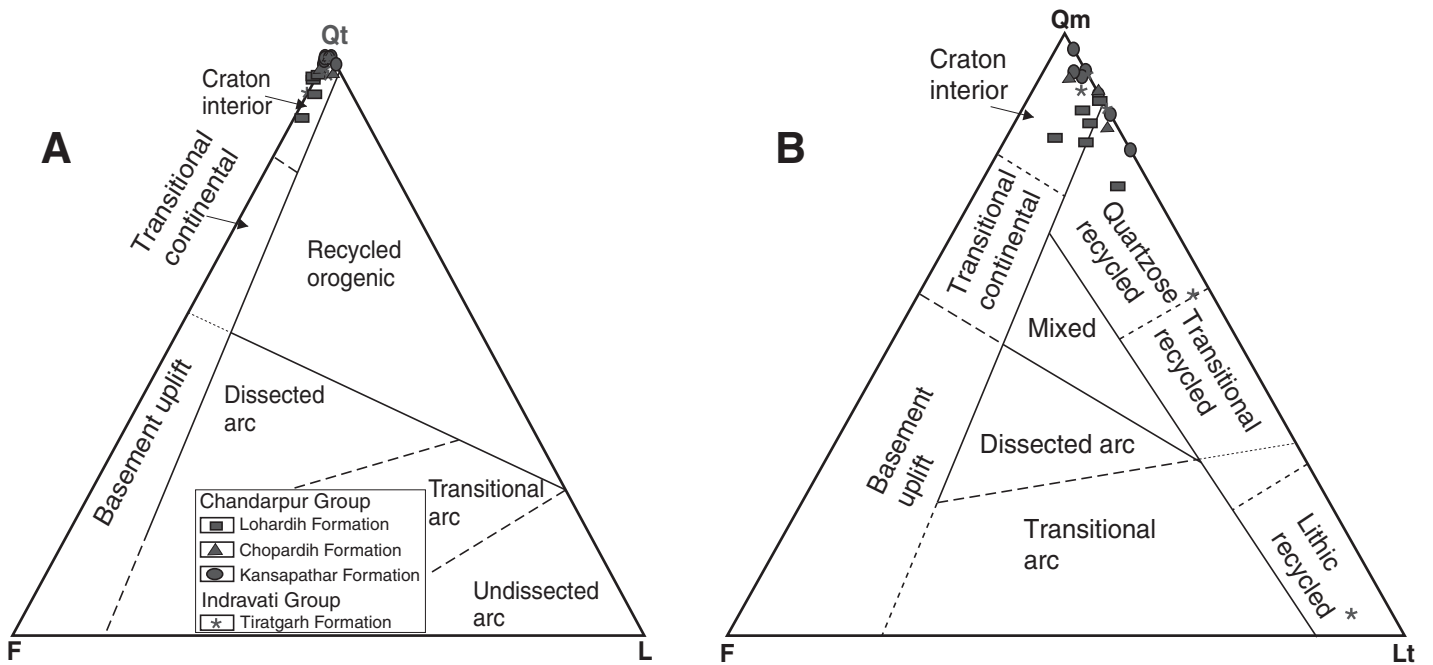


Figure 5. Provenance discrimination diagrams after Dickinson and Suczek (1979): (A) QtFL diagram and (B) QmFLt diagram of the sandstone samples of the Chandarpur Group of the Chhattisgarh Basin and the Tiratgarh Formation of the Indravati Basin.

the craton interior field. In the QmFLt diagram (Dickinson and Suczek, 1979) (Fig. 5B), the majority of the samples of all three formations of the Chandarpur Group and the Tiratgarh Formation of the Indravati Group plot in the craton interior provenance field; however, some samples plot on or near the quartzose recycled orogen. It is evident from QmFLt and QtFL plots that the sandstone samples from all three formations of the Chandarpur Group of the Chhattisgarh Basin, and the Tiratgarh Formation of the Indravati Basin, plot in the intracratonic field.

When combined, the chemical approach and petrographic analysis become a powerful tool for examination of provenance and determination of tectonic setting of a sedimentary basin. Some authors have described the usefulness of major-element geochemistry of sedimentary rocks to infer tectonic setting based on discrimination diagrams (Bhatia, 1983; Roser and Korsch, 1986), although others have pointed out the difficulties in using geochemistry to interpret tectonic setting (Armstrong-Altrin and Verma, 2005; Milodowski and Zalasiewicz, 1991; Nesbitt and Young, 1989; Van de Kamp and Leake, 1985). On the  $\text{SiO}_2$  versus  $\text{K}_2\text{O}/\text{Na}_2\text{O}$  ratio diagram of Roser and Korsch (1986) (Fig. 6A), all the noncalcareous and calcareous shale samples plot exclusively in the PM (passive margin) field. According to Roser and Korsch (1986), PM sediments are quartz-rich sediments derived from plate interiors or stable continental areas that were deposited in intracratonic basins or passive continental margins. Intracratonic basins are formed on a thick continental crust and are included in the passive-margin type tectonic setting (Bhatia, 1983). Hence, in the present case, the terms intracratonic tectonic setting and passive-margin tectonic setting are interchangeable and interrelated; therefore, both terms can be used to represent a single stable tectonic setting. A similar plot to that of the  $\text{K}_2\text{O}/\text{Na}_2\text{O}$  versus  $\text{SiO}_2$  diagram (Roser and Korsch, 1986) was used by Maynard et al. (1982) in their study of modern sand. Modern sands of known tectonic settings exhibit systematic variations in framework mineralogy and chemistry as a function of provenance type and tectonic setting (Valloni and Maynard, 1981). Thus, the composition of modern sedimentary rocks is useful for recognizing the nature of ancient continental margins and ocean basins (Bhatia, 1983). The  $\text{SiO}_2/\text{Al}_2\text{O}_3$  versus  $\text{K}_2\text{O}/\text{Na}_2\text{O}$  plot (Maynard et al., 1982) (Fig. 6B) for the calcareous and noncalcareous shale samples further suggests that the sediments were deposited in a passive-margin setting. Trace elements, particularly those with relatively low mobility and low residence times in seawater, such as Th, Sc, Ti, Nb, and Zr, are transferred quantitatively into clastic sediments during primary weathering and transportation and are thus useful tools for provenance and tectonic setting discrimination (Bhatia and Crook, 1986; McLennan, 1989; McLennan and Taylor, 1991; Taylor and McLennan, 1985). On the Th-Sc-Zr/10 diagram of Bhatia and Crook (1986) (Fig. 7), the calcareous and noncalcareous shale samples of the Chhattisgarh and Indravati Basins plot near the active continental margin and continental arc fields, which is contradictory to the results of the major-element analysis (Fig. 6). The wide scattering of the noncalcareous and calcareous shale samples between active continental margin and continental arc field on the Th-Sc-Zr/10 plot (Fig. 7) may be due to the effect of sorting. According to Roser and Korsch (1986), interpretation of many immobile elements (e.g., Th and Zr) is hampered by their residence in high-density accessory minerals such as zircon and apatite, which may not be necessarily evenly distributed throughout the sediments. So, characteristic geochemical signatures may be difficult to determine using trace elements (Roser and Korsch, 1986).

Therefore, we infer from the petrography of the sandstones and major-element geochemistry of the shales that a stable and intracratonic tectonic setup existed during the deposition of the Chhattisgarh and Indravati sediments. Ash-flow tuffs intercalated with the Gunderdehi shale of the Chhattisgarh Basin, as reported by Chaudhuri et al. (1999), point to intrabasinal

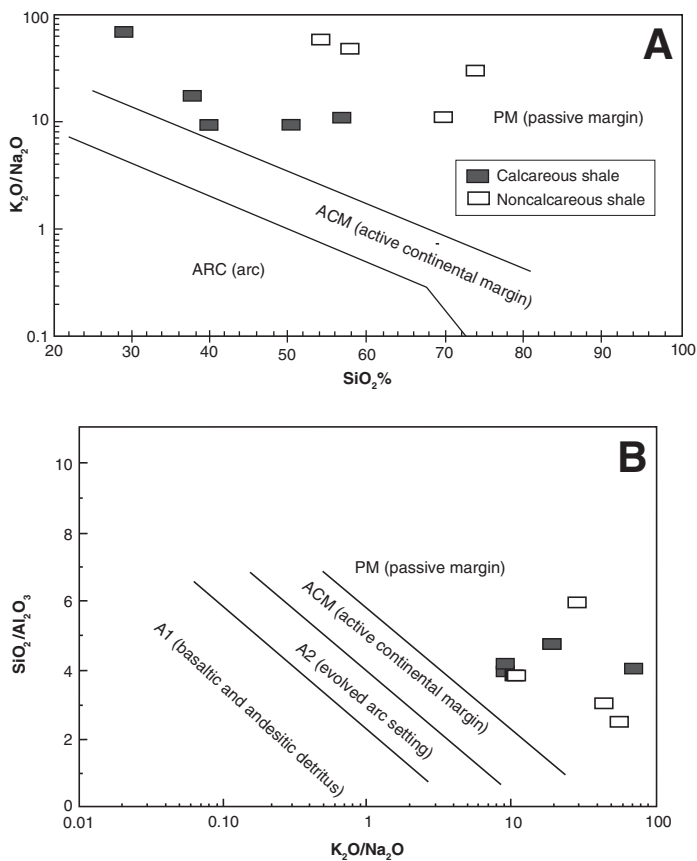


Figure 6. Tectonic setting discrimination diagrams (A)  $\text{K}_2\text{O}/\text{Na}_2\text{O}$  versus  $\text{SiO}_2$  diagram (Roser and Korsch, 1986) and (B)  $\text{SiO}_2/\text{Al}_2\text{O}_3$  versus  $\text{K}_2\text{O}/\text{Na}_2\text{O}$  diagram (Maynard et al., 1982) showing the distribution of the calcareous and noncalcareous shales.

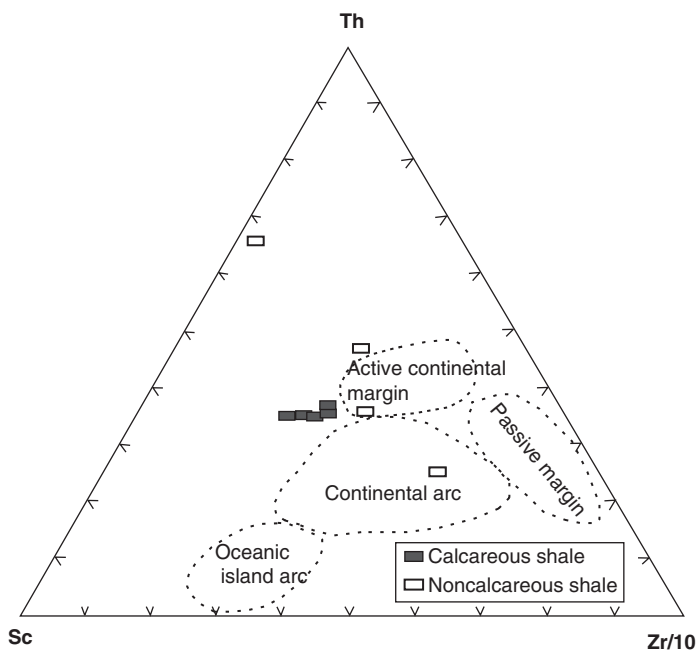


Figure 7. Th-Sc-Zr/10 tectonic discrimination diagram for the calcareous and noncalcareous shales, after Bhatia and Crook (1986).



volcanism or local instability. However, overall, the passive-margin tectonic setting of the Chhattisgarh and Indravati Basins indicates stability of the Bastar craton in the Mesoproterozoic–Neoproterozoic. The stable environment is also indicated by the uniform patterns of stromatolites (lateral linked hemispheroidal stromatolites and stacked hemispheroidal stromatolites; Logan et al., 1964) over extensive areas of the Chhattisgarh and Indravati Basins (Murthi, 1987). In the Bundelkhand and the Bastar blocks, tectonothermal reactivations appear to have ceased by the Neoproterozoic. However, in the Indian Peninsula, several radiometric data indicate major thermal/tectonic events around 1000–941 Ma in the Satpura mobile belt in the Bastar craton (Sarkar, 1983). The Satpura orogeny, which is believed to have been contemporaneous with the Grenville orogeny (Chaudhuri et al., 1999), deformed the Paleoproterozoic Sakoli and Sausar Basins of the Bastar craton (Volpe and Macdougall, 1990). Therefore, it is evident that sedimentation in the undeformed and unmetamorphosed Mesoproterozoic–Neoproterozoic basins has mostly occurred after the Grenville orogeny.

### Provenance

The similarities in the mineralogy of the sandstone samples of the Chandrapur Group and the Tiratgarh Formation, which form the lower parts of the Chhattisgarh and Indravati Basins, respectively, do not reflect any change in the provenance for these sandstones. In the QtFL and QmFLt ternary diagrams (Dickinson and Suczek, 1979) (Fig. 5), all the sandstone samples of the Chandrapur Group of the Chhattisgarh Basin and the Tiratgarh Formation of the Indravati Basin plot in the stable cratonic field, and the samples also suggest craton interior provenance. However, a few samples plot on or near quartzose recycled provenance. According to Dickinson (1985), the main sources for the craton-derived quartzose sands are low-lying granitic and gneissic exposures, supplemented by recycling of associated flat-lying sediments. The mineralogy of these sandstones, such as high quartz content and presence of K-feldspar, is also consistent with their derivation from granitic and gneissic sources.

In comparison, the NASC, LILEs like Rb, Sr, Cs, and Ba, and HFSEs like Ta, Nb, and Th, which are believed to be enriched in felsic source rocks (Feng and Kerrich, 1990), have higher values for the calcareous and the noncalcareous shales. However, compatible elements like transition elements, which are believed to be enriched in mafic source rocks, e.g., Sc, Ni, Cr, and Co, have lower values in both the calcareous and the noncalcareous shales compared to the NASC. This general geochemical trend indicates that felsic sources were dominant during the deposition of the calcareous and noncalcareous shales, and also implies that the source rocks were felsic in composition and evolved similar to the NASC.

Generally, it is believed that post-Archean shales have smaller concentrations of mafic elements, particularly Ni and Cr, when compared to Archean crust (McLennan et al., 1983). On the Ni–Cr diagram (Taylor and McLennan, 1985) (Fig. 8), it is evident that both the calcareous and noncalcareous shales fall in the post-Archean field, which again indicates their derivation from a felsic source. It should be noted here that the noncalcareous shales that are depleted in Ni and Cr are enriched in  $\text{Fe}_2\text{O}_3$  (7.39%) compared to NASC (Fig. 3). The higher  $\text{Fe}_2\text{O}_3$  in the noncalcareous shales can be due to derivation of Fe from Fe-rich chemical precipitates derived from the Archean banded iron formation of the Bastar craton.

Contrary to the Archean, the post-Archean sedimentary rocks are generally enriched in LREEs, depleted in HREEs, and have  $\text{Eu}/\text{Eu}^* < 1$  and  $(\text{Gd}/\text{Yb})_n < 2$  (McLennan et al., 1993). When the calcareous shales are compared to the noncalcareous shales, the latter have higher  $\Sigma\text{REE}$  abundances (Table 3). The REE patterns of both the calcareous and the noncalcareous shales show LREE enrichment, flat HREE, and a negative

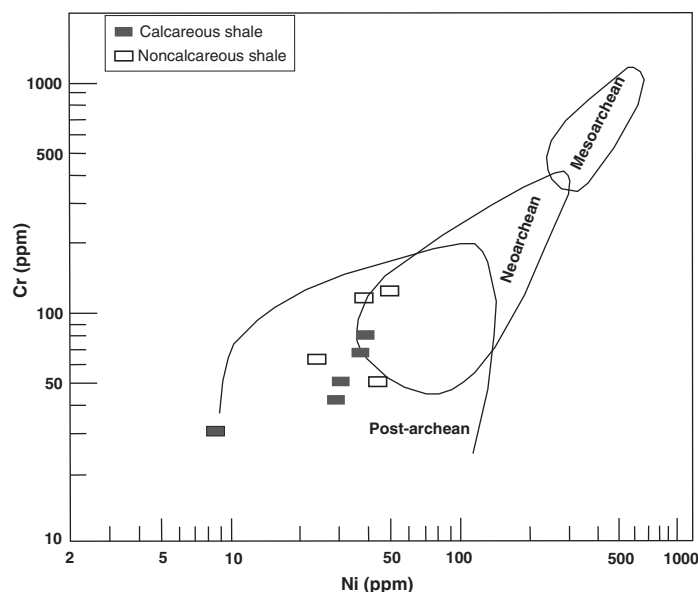


Figure 8. Distribution of Ni and Cr in the calcareous and noncalcareous shales. Different types of rocks are also shown for comparison. Fields are after Condie (1993).

Eu anomaly. The  $\text{Eu}/\text{Eu}^*$  value of the noncalcareous shales is close to the  $\text{Eu}/\text{Eu}^*$  value of the granite (0.40) and gneiss (0.65) of the Bastar craton (Mondal et al., 2006). The higher  $\text{Eu}/\text{Eu}^*$  value (1.1) of the sample (RD-512) of calcareous shales suggests that it might have source rock like basalt or tonalite. The Bastar gneisses, which are tonalitic in composition (Hussain et al., 2004), might be the source rock rather than basalt, as this sample is depleted in transition elements. It is also evident from the chondrite-normalized (Sun and McDonough, 1989) REE patterns (Fig. 9) that both the calcareous and noncalcareous shales have REE patterns similar to the granite and gneiss (Mondal et al., 2006) of the Bastar craton and do not match with the REE patterns of the Archean mafic volcanic rocks

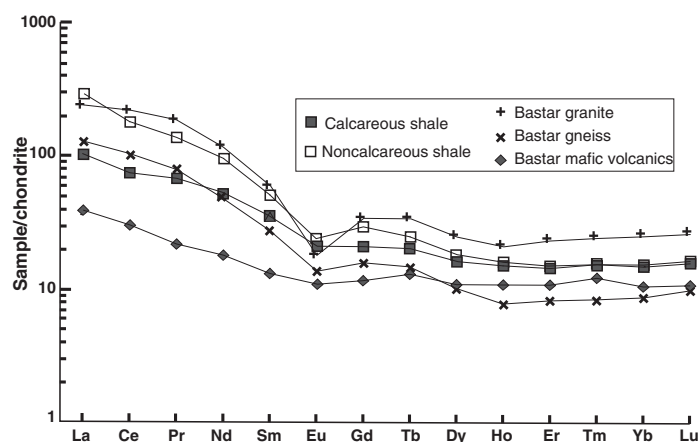


Figure 9. Chondrite-normalized (Sun and McDonough, 1989) rare earth element (REE) patterns of the calcareous and noncalcareous shales. Chondrite-normalized REE patterns of the granite, gneiss, and mafic volcanic rocks are shown for comparison. Data for the granite and gneiss of the Bastar craton are from Mondal et al. (2006), and data for mafic volcanic rocks are from Srivastava et al. (2004).

(Srivastava et al., 2004) of the Bastar craton. Further, it is considered that the REEs generally reside in minerals like zircon and allanite (McLennan, 1989). The positive correlation between REE and Zr in the calcareous shales ( $r = 0.9$ ) and between REE and Th in the noncalcareous shales ( $r = 0.91$ ) suggests that the REEs in noncalcareous shales and calcareous shales are controlled by zircon and allanite, which are accessory minerals in the granitoids. The REE budget in clastic sedimentary rocks is chiefly controlled by granitoids (Jahn and Condie, 1995).

The elemental concentrations of the calcareous shales are lower than those of the noncalcareous shales due to calcite dilution in the former. So, we infer that the elemental concentrations of the calcareous shales should deviate from the source rock. However, elemental ratios of the immobile trace elements in these calcareous shales may be more representative of the source than their elemental concentrations (Cullers, 2000; Cullers and Podkovyrov, 2002). To evaluate the extent to which the elemental ratios vary with calcite dilution in the calcareous shales, we plotted certain key elemental ratios like Th/Co, Th/Sc, La/Sc, La/Co, Ni/Cr, Cr/Th, Eu/Eu\*, and (Gd/Yb)<sub>n</sub> of the calcareous shales against CaO% (Figs. 10A and 10B). It is evident from the plot that these elemental ratios do not vary over a range of CaO% in the calcareous shales. Thus, these ratios are not affected by calcite dilution in the calcareous shales. Therefore, this study attests the importance of these elemental ratios in determining source rock characteristics of the calcareous shales and the noncalcareous shales.

To further understand the nature of the provenance of the calcareous shales and the noncalcareous shales, we normalized different key elemental ratios like (La/Yb)<sub>n</sub>, LREE/HREE, La/Sc, Th/Sc, La/Co, Th/Co, Sc/Cr, Sc/Ni, (Gd/Yb)<sub>n</sub>, Th/U, Zr/Hf, Zr/Th, La/Th, and also the Eu/Eu\* ratio of these calcareous and noncalcareous shales with those of the UCC. It is evident from the Figures 11A and 11B that most of the key elemental ratios of the calcareous and the noncalcareous shales that are thought to be characteristic for provenance determination are similar or show very little

variation as compared to UCC, suggesting that both the calcareous and the noncalcareous shales were derived from the evolved source similar to the UCC. Overall, the petrology of the sandstones (which form stratigraphically the lower parts) and the geochemistry of the shales (which form stratigraphically the upper parts) of the Chhattisgarh and Indravati Basins indicate homogeneity in the source rock composition (felsic rocks) during the Mesoproterozoic–Neoproterozoic. The source rocks have been found to be felsic in nature and are identified to be the granites and gneisses of the Bastar craton.

### Paleoredox Conditions

Knowledge about paleoredox conditions is essential for reconstructing the way in which the oxygenation of Earth's surface environment has changed through time and affected the evolution of life on our planet (Severmann and Anbar, 2009). The ratio Ce/Ce\* has been used in sedimentary rocks to interpret the redox conditions in seawater at the time when the REEs were incorporated into the marine sediment (German and Elderfield, 1990). Ce may oxidize in seawater from the 3+ to the more insoluble 4+ oxidation state, thus enriching the sediment in Ce relative to the other REEs (Bellanca et al., 1997; German and Elderfield, 1990; Cullers, 2002). The calcareous shales analyzed in this study contain lower Ce/Ce\* (average 0.86) (Table 3) compared to the noncalcareous shales (0.93). Present seawater is characterized by Ce/Ce\* values of 0.4–0.7 (Table 3) (Elderfield and Greaves, 1982), whereas the average shales typically yield Ce/Ce\* values of ~1.0 (Cox et al., 1995; Cullers and Berendsen, 1998). Therefore, the Ce/Ce\* values of calcareous shales are slightly lower compared to the noncalcareous shales and slightly higher compared to those of present ocean water. This indicates suboxic conditions for the calcareous shales and oxic conditions for the noncalcareous shales. The Mn\* value has also been used by a number of workers as a paleochemical indicator

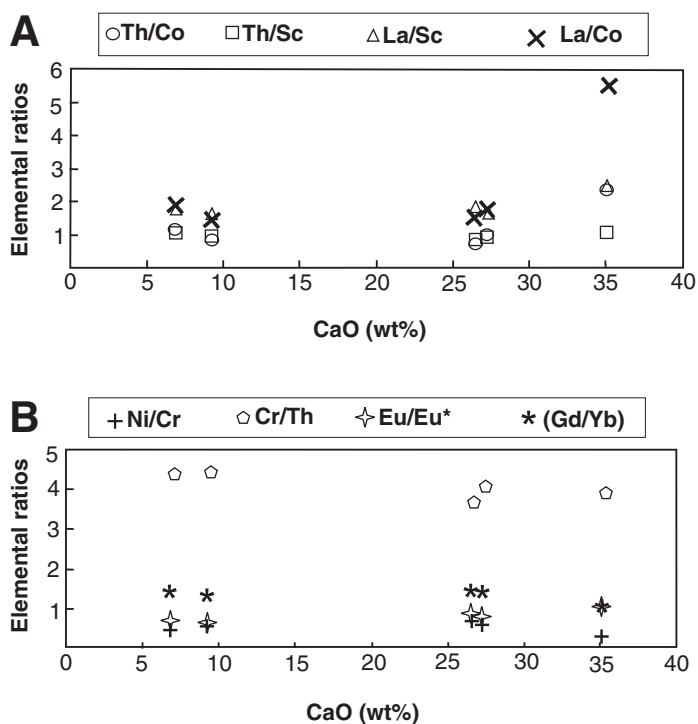


Figure 10. Plots of CaO versus elemental ratios of calcareous shales (A) Th/Co, Th/Sc, La/Sc and La/Co; and (B) Ni/Cr, Cr/Th, Eu/Eu\*, and (Gd/Yb)<sub>n</sub>.

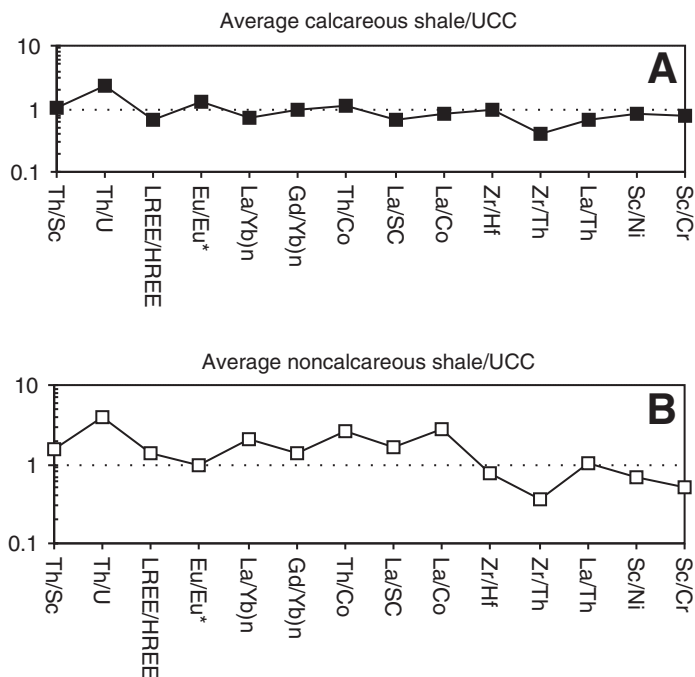


Figure 11. Upper continental crust (UCC)-normalized elemental ratios Th/Sc, Th/U, LREE/HREE (light to heavy rare earth element ratio), Eu/Eu\*, (La/Yb)<sub>n</sub>, (Gd/Yb)<sub>n</sub>, Th/Co, La/Sc, La/Co, Zr/Hf, Zr/Th, La/Th, Sc/Ni, and Sc/Cr for the (A) calcareous and (B) noncalcareous shales.

of the redox conditions of the depositional environment (Bellanca et al., 1996; Cullers, 2002; Machhour et al., 1994). The  $Mn^*$  value can be calculated as:  $Mn^* = \log \left( \frac{[Mn_{\text{sample}}/Mn_{\text{shales}}]}{[Fe_{\text{sample}}/Fe_{\text{shales}}]} \right)$ .

The values used for  $Mn_{\text{shales}}$  and  $Fe_{\text{shales}}$  are 600 ppm and 46,150 ppm, respectively (Wedepohl, 1978). The manganese tends to accumulate in more oxygenated conditions above the redox boundary (Bellanca et al., 1996). Thus, the less positive  $Mn^*$  values for the calcareous shales suggest that they were mostly formed in suboxic conditions. The noncalcareous shales with the highest  $Ce/Ce^*$  values (0.93) have negative  $Mn^*$  values (average  $-0.68$ ), again suggesting that the noncalcareous shales may have been deposited in oxic conditions. The inverse correlation of the  $Ce/Ce^*$  values and  $Mn^*$  values in the calcareous shales suggests that redox of  $Ce$  was linked with that of  $Mn$  and  $Fe$ .

These interpretations are consistent with the presence of glauconites in the calcareous shales (Gunderdehi shales) (Murthi, 1987). The glauconites are well developed mostly in suboxic environments (Kelly and Webb, 1999). The pink color of the calcareous shales (Gunderdehi shales) may further support formation in a suboxic environment. This indicates that the Chhattisgarh and Indravati Basins must have experienced fluctuations between oxidizing and reducing environments, probably due to the sea-level change.

## CONCLUSIONS

The petrology of sandstones and the geochemistry of the shales of the Mesoproterozoic–Neoproterozoic Chhattisgarh and Indravati Basins indicate homogeneity in the source rock composition. The sandstone petrology suggests that sediments were derived from granite and gneiss of a continental block or intracratonic tectonic setting. The geochemistry of shales suggests that the sediments were mainly derived from felsic rocks, and the source rocks have been identified as the Archean granites and gneisses of the Bastar craton. The study also points to the absence of mafic rocks in the provenance during the Mesoproterozoic–Neoproterozoic or their complete removal before the sedimentation in the Chhattisgarh and Indravati Basins of the Bastar craton. The study suggests that sedimentation in the Chhattisgarh and Indravati Basins took place in passive or intracratonic tectonic settings. This indicates stability of the Bastar craton in particular, and peninsular India in general, and also suggests that the Indian peninsula was set for intraplate tectonics in the Mesoproterozoic–Neoproterozoic. The  $Ce/Ce^*$  values and  $Mn^*$  values of the calcareous shales and the noncalcareous shales suggest that the Chhattisgarh and Indravati Basins must have experienced fluctuations between oxidizing and reducing environments.

## ACKNOWLEDGMENTS

We are thankful to the chairman, Department of Geology, Aligarh Muslim University, Aligarh, for providing the facilities to carry out this work. We also wish to express sincere thanks to the director of the Wadia Institute of Himalayan Geology, Dehradun, and V. Balram, head of the Geochemistry Division, National Geophysical Research Institute (NGRI), Hyderabad, for providing laboratory facilities during chemical analysis. H. Wani also thanks the principal, Government Amar Singh College, Srinagar, for encouragement and help during this work and thankfully acknowledges a Council of Scientific and Industrial Research (CSIR) fellowship grant, government of India. We thank James P. Evans and Jon D. Pelletier for their editorial handling. We also thank P. Erikson, R. Cullers, and an anonymous reviewer for their constructive comments on the manuscript.

## REFERENCES CITED

- Armstrong-Altrin, J.S., and Verma, S.P., 2005, Critical evaluation of six tectonic setting discrimination diagrams using geochemical data of Neogene sediments from known tectonic settings: *Sedimentary Geology*, v. 177, p. 115–129, doi:10.1016/j.sedgeo.2005.02.004.
- Bandopadhyaya, B.K., Roy, A., and Huin, A.K., 1995, Structure and tectonics of a part of the Central Indian Shield, in Roy, S.S., and Gupta, K.R., eds., *Continental Crust of North-western and Central India: Geological Society of India Memoir 31*, p. 433–468.
- Bellanca, A., Claps, M., Erba, E., Masetti, D., Neri, R., Premoli-Silva, I., and Venezia, F., 1996, Orbitally induced limestone/marlstone rhythms in the Albian-Cenomanian Cison section (Venetian region, northern Italy): *Sedimentology, calcareous and siliceous plankton distribution, elemental and isotope geochemistry: Palaeogeography, Palaeoclimatology, Palaeoecology*, v. 126, p. 227–260, doi:10.1016/S0031-0182(96)00041-7.
- Bellanca, A., Masetti, D., and Neri, R., 1997, Rare earth elements in limestone/marlstone couplets from the Albanian-Cenomanian Cison section (Venetian region, northern Italy): *Assessing REE sensitivity to environmental changes: Chemical Geology*, v. 141, p. 141–152, doi:10.1016/S0009-2541(97)00058-2.
- Bhat, M.I., and Ghosh, S.K., 2001, Geochemistry of the 2.51 Ga old Rampur Group pelites, western Himalayas: Implications for their provenance and weathering: *Precambrian Research*, v. 108, p. 1–16, doi:10.1016/S0301-9268(00)0139-X.
- Bhatia, M.R., 1983, Plate tectonics and geochemical composition of sandstones: *The Journal of Geology*, v. 91, p. 611–627, doi:10.1086/628815.
- Bhatia, M.R., and Crook, K.A.W., 1986, Trace element characteristics of greywackes and tectonic discrimination of sedimentary basins: *Contributions to Mineralogy and Petrology*, v. 92, p. 181–193, doi:10.1007/BF00375292.
- Blatt, H., 1967, Provenance determinations and recycling of sediments: *Journal of Sedimentary Petrology*, v. 37, p. 1311–1320.
- Cawood, P.A., Kröner, A., and Pisarevsky, S., 2006, Trace element characteristics for provenance: *Criteria and evidence: GSA Today*, v. 16, no. 7, p. 4–11, doi:10.1130/GSAT01607.1.
- Chaudhuri, A.K., Mukhopadhyay, J., Patranabis Deb, S., and Chanda, S.K., 1999, The Neoproterozoic successions of peninsular India: *Gondwana Research*, v. 2, p. 213–225, doi:10.1016/S1342-937X(05)70146-5.
- Chaudhuri, A.K., Saha, D., Deb, G.K., Deb, S.P., Mukherji, M.K., and Ghosh, G., 2002, The Purana basins of southern cratonic province of India—A case for Mesoproterozoic fossil rifts: *Gondwana Research*, v. 5, p. 23–33, doi:10.1016/S1342-937X(05)70884-4.
- Condie, K.C., 1993, Chemical composition and evolution of the upper continental crust: Contrasting results from surface samples and shales: *Chemical Geology*, v. 104, p. 1–37.
- Cox, R., Low, D.R., and Cullers, R.L., 1995, The influence of sediment recycling and basement composition on evolution of mud rock chemistry in the southwestern United States: *Geochimica et Cosmochimica Acta*, v. 59, p. 2919–2940, doi:10.1016/0016-7037(95)0185-9.
- Cullers, R.L., 2000, The geochemistry of shales, siltstones and sandstones of Pennsylvanian-Permian age, Colorado, USA: Implications for provenance and metamorphic studies: *Lithos*, v. 51, p. 181–203, doi:10.1016/S0024-4937(99)00063-8.
- Cullers, R.L., 2002, Implications of elemental concentrations for provenance, redox conditions, and metamorphic studies of shales and limestones near Pueblo, Co, USA: *Chemical Geology*, v. 191, p. 305–327, doi:10.1016/S0009-2541(02)00133-X.
- Cullers, R.L., and Berendsen, P., 1998, The provenance and chemical variation of sandstones associated with the Mid-Continent Rift system, USA: *European Journal of Mineralogy*, v. 10, p. 987–1002.
- Cullers, R.L., and Podkovyrov, V.N., 2002, The source and origin of terrigenous sedimentary rocks in the Mesoproterozoic Uj Group, southeastern Russia: *Precambrian Research*, v. 117, p. 157–183, doi:10.1016/S0301-9268(02)00079-7.
- Dickinson, W.R., 1970, Interpreting detrital modes of greywacke and arkose: *Journal of Sedimentary Petrology*, v. 40, p. 695–707.
- Dickinson, W.R., 1985, Interpreting provenance relations from detrital modes of sandstones, in Zuffa, G.G., ed., *Provenance of Arenites: Dordrecht, D. Reidel*, p. 333–362.
- Dickinson, W.R., and Suczek, C.A., 1979, Plate tectonics and sandstone compositions: *American Association of Petroleum Geologists Bulletin*, v. 63, p. 2164–2182.
- Elderfield, H., and Greaves, M.J., 1982, The rare earth elements in sea-water: *Nature*, v. 296, p. 214–219, doi:10.1038/296214a0.
- Eriksson, K.A., Taylor, S.R., and Korsch, R.J., 1992, Geochemistry of 1.8–1.67 Ga mudstones and siltstones from the Mount Isa Inlier, Queensland, Australia: Provenance and tectonic implications: *Geochimica et Cosmochimica Acta*, v. 56, p. 899–909, doi:10.1016/0016-7037(92)90035-H.
- Eriksson, P.G., Condie, K.C., Vander, W., Vander, M., DeBruyn, H., Nelson, D.R., Altermann, W., Catuneanu, O., Bumby, A.J., Lindsay, J., and Cunningham, M.J., 2002, Late Archean superplume events, a Kaapvaal-Pilbara perspective: *Journal of Geodynamics*, v. 34, p. 207–247, doi:10.1016/S0264-3707(02)00022-4.
- Feng, R., and Kerrich, R., 1990, Geochemistry of fine grained clastic sediments in the Archean Abitibi greenstone belt, Canada: Implications for provenance and tectonic setting: *Geochimica et Cosmochimica Acta*, v. 54, p. 1061–1081, doi:10.1016/0016-7037(90)90439-R.
- Folk, R.L., 1980, *Petrology of Sedimentary Rocks*: Austin, Texas, Hemphill Publishing Co., 182 p.
- German, C.R., and Elderfield, H., 1990, Application of the Ce anomaly as a paleoredox indicator: The ground rules: *Paleoceanography*, v. 5, p. 823–833, doi:10.1029/PA005i05p0823.
- Gromet, L.P., Dymek, R.F., Haskin, L.A., and Korotev, R.L., 1984, The “North American shale composite”: Its compilation, major and trace element characteristics: *Geochimica et Cosmochimica Acta*, v. 48, p. 2469–2482, doi:10.1016/0016-7037(84)90298-9.
- Holland, T.H., 1907, *Geology: Imperial Gazetteer of India*, Government of India Delhi, v. 1, p. 50–103.
- Hussain, M.F., Mondal, M.E.A., and Ahmad, T., 2004, Petrological and geochemical characteristics of Archean gneisses and granitoids from Bastar craton, central India—Implication

- for subduction related magmatism: *Gondwana Research*, v. 7, p. 531–537, doi:10.1016/S1342-937X(05)70803-0.
- Ingersoll, R.V., Bullard, T.F., Ford, R.L., Grimm, J.P., Pickle, J.D., and Sares, S.W., 1984, The effect of grain size on detrital modes: A test of Gazzi-Dickinson point-counting method: *Journal of Sedimentary Petrology*, v. 54, p. 103–116.
- Jahn, B.M., and Condie, K.C., 1995, Evolution of the Kaapvaal craton as viewed from geochemical and Sm-Nd isotopic analyses of intra-cratonic pelites: *Geochimica et Cosmochimica Acta*, v. 59, p. 2239–2258, doi:10.1016/0016-7037(95)00103-7.
- Kale, V.S., and Phansalkar, V.G., 1991, Purana basins of peninsular India: A review: *Basin Research*, v. 3, p. 1–36, doi:10.1111/j.1365-2117.1991.tb00133.x.
- Kelly, J.C., and Webb, J.A., 1999, The genesis of glaucony in the Oligo-Miocene Torquay Group southeastern Australia: Petrographic and geochemical evidence: *Sedimentary Geology*, v. 125, p. 99–114, doi:10.1016/S0037-0738(98)00149-3.
- Le Gazzi, P., 1966, Arenarie del flysch sopracretaceo dell'Appennino modenese; correlazioni con il flysch di Monghidoro: *Mineralogica Petrographica Acta*, v. 12, p. 69–97.
- Logan, B.W., Rezak, R., and Ginsburg, R.N., 1964, Classification and environmental significance of algal stromatolites: *The Journal of Geology*, v. 72, p. 68–83, doi:10.1086/626965.
- Machhour, L., Philip, J., and Oudin, J.L., 1994, Formation of laminate deposit in anaerobic-dysaerobic marine environments: *Marine Geology*, v. 117, p. 287–302, doi:10.1016/0025-3227(94)90021-3.
- Maynard, J.B., Valloni, R., and Yu, H., 1982, Composition of modern deep sea sands from arc-related basins, in Leggett, J.K., ed., *Trench-forearc geology*: Geological Society of London Special Publication 10, p. 551–561, doi:10.1144/GSL.SP.1982.010.01.36.
- McCulloch, M.T., and Wasserburg, G.J., 1978, Sm-Nd and Rb-Sr chronology of continental crust formation: *Science*, v. 200, p. 1003–1011, doi:10.1126/science.200.4345.1003.
- McLennan, S.M., 1989, Rare earth elements in sedimentary rocks: Influence of provenance and sedimentary process, in Lipin, B.R., and McKay, G.A., eds., *Geochemistry and Mineralogy of Rare Earth Elements: Reviews in Mineralogy*, v. 21, p. 169–200.
- McLennan, S.M., and Taylor, S.R., 1991, Sedimentary rocks and crustal evolution: Tectonic setting and secular trends: *The Journal of Geology*, v. 99, p. 1–21, doi:10.1086/629470.
- McLennan, S.M., Taylor, S.R., and Eriksson, K.A., 1983, Geochemistry of Archean shales from the Pilbara Supergroup, Western Australia: *Geochimica et Cosmochimica Acta*, v. 47, p. 1211–1222, doi:10.1016/0016-7037(83)90063-7.
- McLennan, S.M., Hemming, S., McDaniel, D.K., and Hanson, G.N., 1993, Geochemical approaches to sedimentation, provenance and tectonics, in Johnsson, M.J., and Basu, A., eds., *Processes Controlling the Composition of Clastic Sediments*: Geological Society of America Special Paper 284, p. 21–40.
- Milodowski, A.E., and Zalasiewicz, J.A., 1991, Redistribution of rare earth elements during diagenesis of turbidite/hemipelagic mudrock sequences of Llandovery age from central Wales, in Morton, A.C., Todd, S.P., and Haughton, P.D.W., eds., *Developments in Sedimentary Provenance Studies*: Geological Society of America Special Publication 57, p. 101–124.
- Mondal, M.E.A., Hussain, M.F., and Ahmad, T., 2006, Continental growth of Bastar craton, Central Indian Shield during Precambrian via multiphase subduction and lithospheric extension/rifting: Evidence from geochemistry of gneisses, granitoids and mafic dykes: *Journal of Geosciences, Osaka City University*, v. 49, p. 137–151.
- Murthi, K.S., 1987, Stratigraphy and sedimentation in Chhattisgarh Basin, in Radhakrishna, B.P., ed., *Purana Basins of Peninsular India*: Geological Society of India Memoir 6, p. 239–260.
- Naqvi, S.M., and Rogers, J.J.W., 1987, *Precambrian Geology of India*: New York, U.S.A., Oxford University Press, 223 p.
- Nesbitt, H.W., and Young, G.M., 1989, Formation and diagenesis of weathering profiles: *The Journal of Geology*, v. 97, p. 129–147, doi:10.1086/629290.
- Patranabis Deb, S., 2004, Lithostratigraphy of the Neoproterozoic Chhattisgarh sequence; its bearing on the tectonics and paleogeography: *Gondwana Research*, v. 7, p. 323–337, doi:10.1016/S1342-937X(05)70787-5.
- Pettijohn, F.J., Potter, P.E., and Siever, R., 1972, *Sand and Sandstone*: Berlin, Springer-Verlag, 618 p.
- Preiss, W.V., and Forbes, B.G., 1981, Stratigraphy, correlation and sedimentary history of Adelaidean (Late Proterozoic) basins of Australia: *Precambrian Research*, v. 15, p. 255–304, doi:10.1016/0301-9268(81)90054-1.
- Radhakrishna, B.P., 1989, Suspect tectono-stratigraphic terrane elements in the Indian sub-continent: *Journal of the Geological Society of India*, v. 34, p. 1–24.
- Ramakrishnan, M., 1987, Stratigraphy, sedimentary environment and evolution of the Late Proterozoic Indravati Basin, Central India, in Radhakrishna, B.P., ed., *Purana Basins of Peninsular India*: Geological Society of India Memoir 6, p. 139–160.
- Rogers, J.J.W., 1986, The Dharwar craton and the assembly of peninsular India: *The Journal of Geology*, v. 94, p. 129–143, doi:10.1086/629019.
- Roser, B.P., and Korsch, R.J., 1986, Determination of tectonic setting of sandstone-mudstone suites using SiO<sub>2</sub> content and K<sub>2</sub>O/Na<sub>2</sub>O ratio: *The Journal of Geology*, v. 94, p. 635–650, doi:10.1086/629071.
- Roy, P., Balam, V., Kumar, A., Satyanarayanan, M., and Rao, G., 2007, New REE and trace element data on two international kimberlitic reference materials by ICP-MS: *Journal of Geostandards and Geoanalytical Research*, v. 31, p. 261–273, doi:10.1111/j.1751-908X.2007.00836.x.
- Saini, N.K., Mukherjee, P.K., Rathi, M.S., Khanna, P.P., and Purohit, K.K., 1998, A new geochemical reference sample of granite (DG-H) from Dalhousie, Himachal Himalaya: *Journal of the Geological Society of India*, v. 52, p. 603–606.
- Sarkar, S., 1983, Present status of Precambrian stratigraphy and geochronology of peninsular India—A synopsis: *Indian Journal of Earth Sciences*, v. 10, p. 104–106.
- Severmann, S., and Anbar, A.D., 2009, Reconstructing paleoredox conditions through a multi-tracer approach: The key to the past is the present: *Elements*, v. 5, p. 359–364.
- Srivastava, R.K., Singh, R.K., and Verma, S.P., 2004, Neoproterozoic mafic volcanic rocks from the southern Bastar greenstone belt, central India: Petrological and tectonic significance: *Precambrian Research*, v. 131, p. 305–322, doi:10.1016/j.precamres.2003.12.013.
- Sun, S.S., and McDonough, W.F., 1989, Chemical and isotopic systematics of oceanic basalts: Implications for mantle composition and processes, in Saunderson, A.D., and Norry, M.J., eds., *Magma-tism in Oceanic Basins*: Geological Society of London Special Publication 42, p. 313–345.
- Takashi, K., Yoshida, M., Wada, H., Satish-Kumar, M., Roy, A., Bandhopadhyay, B.K., Khan, A.S., Pal, T., Huin, A.K., Bhowmik, S.K., and Chattopadhyay, A., 2001, Field studies in the Sakoli belts of the Central Indian tectonic zone: *Journal of Geosciences, Osaka City University*, v. 44, p. 17–39.
- Taylor, S.R., and McLennan, S.M., 1985, *The Continental Crust: Its Composition and Evolution*: Oxford, Blackwell, 311 p.
- Valloni, R., and Maynard, J.B., 1981, Detrital modes of recent deep-sea sands and their relation to tectonic setting: A first approximation: *Sedimentology*, v. 28, p. 75–83, doi:10.1111/j.1365-3091.1981.tb01664.x.
- Van de Kamp, P.C., and Leake, B.E., 1985, Petrography and geochemistry of feldspathic and mafic sediments of the northeastern Pacific margin: *Transactions of the Royal Society of Edinburgh—Earth Sciences*, v. 76, p. 411–449.
- Volpe, A.M., and Macdougall, J.D., 1990, Geochemistry and isotopic characteristic of mafic (Phulad ophiolite) and related rocks in the Delhi Supergroup, Rajasthan, India: Implications for rift in the Proterozoic: *Precambrian Research*, v. 48, p. 167–191, doi:10.1016/0301-9268(90)90061-T.
- Wedepohl, K.H., 1978, Manganese: Abundance in common sediments and sedimentary rocks, in Wedepohl, K.H., ed., *Handbook of Geochemistry*: Berlin, Springer, p. 1–17.
- Wronkiewicz, D.J., and Condie, K.C., 1989, Geochemistry and provenance of sediments from the Pongola Supergroup, South Africa: Evidence from a 3.0 Ga-old continental craton: *Geochimica et Cosmochimica Acta*, v. 53, p. 1537–1549, doi:10.1016/0016-7037(89)90236-6.
- Wronkiewicz, D.J., and Condie, K.C., 1990, Geochemistry and mineralogy of sediments from the Ventersdorp and Transvaal Supergroups, South Africa: Cratonic evolution during the early Proterozoic: *Geochimica et Cosmochimica Acta*, v. 54, p. 343–354, doi:10.1016/0016-7037(90)90323-D.

MANUSCRIPT RECEIVED 5 AUGUST 2009

REVISED MANUSCRIPT RECEIVED 18 NOVEMBER 2010

MANUSCRIPT ACCEPTED 6 DECEMBER 2010

Printed in the USA